

High efficiency single-junction semitransparent perovskite solar cells

Supporting information

Cristina Roldán-Carmona,^{†ab} Olga Malinkiewicz,^{†a} Rafael Betancur,^c Giulia Longo,^a Cristina Momblona,^a Franklin Jaramillo,^c Luis Camacho^b and Henk J. Bolink^{*a}

[†] These authors contributed equally to this work

^a Instituto de Ciencia Molecular, Universidad de Valencia, C/ Catedrático J. Beltrán 2, 46980 Paterna (Valencia), Spain. henk.bolink@uv.es

^b Department of Physical Chemistry and Applied Thermodynamics, Campus Rabanales, Ed. C3, University of Cordoba, 14014, Spain.

^c Centro de investigación, innovación y desarrollo de materiales-CIDEMAT, Universidad de Antioquia UdeA, Calle 70 No 52-21, Medellín, Colombia

Email: henk.bolink@uv.es

Content:

1. Methods: materials, device preparation and characterization. (Page 2)
2. Electrode transmittance measurements. (Page 2-3)
3. Perovskite film characterization. (Page 3)
4. Performance of perovskite solar cells with 70nm Au as cathode. (Page 4)
5. Transmittance spectra for optimized device. (Page 4)
6. Chromaticity coordinates for the semitransparent devices (Page 4)

1. Methods

Materials

Aqueous dispersions of poly(3,4-ethylenedioxythiophene) doped with poly(styrenesulfonate) (PEDOT:PSS, CLEVIOS P VP Al 4083) were obtained from Heraeus Holding GmbH and used as received. Poly[N,N'-bis(4-butylphenyl)-N,N'-bis(phenyl)benzidine] (poly-TPD) was purchased from ADS Dyesource. PbI_2 was purchased from Aldrich and used as is, $\text{CH}_3\text{NH}_3\text{I}$ was prepared similar to a previously published method¹, in brief: *$\text{CH}_3\text{NH}_3\text{I}$, was synthesized by reacting 21.6 ml methylamine (40%wt in water, Aldrich) and 30 ml hydroiodic acid (57 wt% in water, Aldrich) in a 250 ml round-bottomed flask at 0 °C for 2 h with stirring. The white precipitate was recovered by evaporation at 50 °C for 1 h. The product, methylammonium iodide ($\text{CH}_3\text{NH}_3\text{I}$), was dissolved in ethanol, filtered and recrystallized from diethyl ether, and dried at 60 °C in a vacuum oven for 24 h.*

Device preparation

Devices were prepared on a photolithographically patterned ITO on glass substrates, by spincoating a thin layer of PEDOT:PSS from the commercial aqueous dispersion (1000rpm 30sec and a short annealing at 150 °C result in 75 nm thickness). On top of this layer a thin film of polyTPD was deposited from a chlorobenzene solution (7 mg ml⁻¹) using spincoating. Then the substrates were annealed at 180 °C during 30 minutes and transferred to a vacuum chamber integrated into an inert glovebox (MBraun, <0.1 ppm O₂ and <0.1 ppm H₂O) and evacuated to a pressure of 1×10^{-6} mbar. The sublimation of the perovskite was performed using a vacuum chamber of MBraun integrated in an inert glovebox (MBraun) as previously reported². The PCBM₆₀ layer was deposited using a chlorobenzene solution of 10 mg ml⁻¹ in ambient conditions using a meniscus coater and a coating speed of 10 mm/ second. The device was completed by the thermal evaporation of the top semitransparent electrode under a base pressure of 2×10^{-6} mbar. The solar cells (active area of 0.12 cm²) were characterized inside the inert glovebox.

Device characterization

Solar cells were illuminated by a white light halogen lamp in combination with interference filters for the EQE and *J-V* measurements (MiniSun simulator by ECN the Netherlands). A black mask with openings matching the active cell area was used to limit the active area of the device. Before each measurement, the exact light intensity was determined using a calibrated Si reference diode. An estimation of the short-circuit current density (J_{sc}) under standard test conditions was calculated by convolving the EQE spectrum with the AM1.5G reference spectrum, using the premise of a linear dependence of J_{sc} on light intensity. Current-voltage (*J-V*) characteristics were measured using a Keithley 2400 source measure unit. All characterization was done in a nitrogen filled glove box (<0.1 ppm O₂ and <0.1 ppm H₂O) without exposure to ambient atmosphere.

2. Electrode transmittance measurements

Different cathodes were prepared in order to use the most appropriate to our cell configuration. All of them consisted on an evaporated mixture of metals, metals and oxides, as well as the lithium fluoride salt. Due to the better performance of our solar cells when using gold as the cathode, it was used as the seed layer in most of the cases. The transmittance of the studied cathodes is shown in Figure S1.

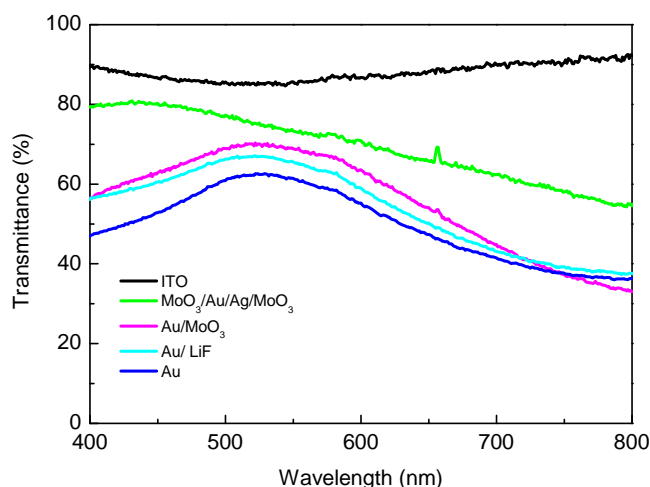


Figure S1. Transmittance spectra for the different semitransparent electrodes. The presence of LiF and MoO₃ increases slightly the transmittance referred to the 6 nm gold. ITO electrode is also included as a reference.

Table S1. Most important parameters of non optimized semitransparent solar cells with the following configuration: ITO/PEDOT:PSS/PolyTPD/Perovskite/PCBM₆₀/ST electrode for an active layer thickness of 250nm.

ST electrode	J_{sc} (mA cm ⁻²)	V_{oc} (V)	FF	PCE (%)	AVT ¹ (%)
Au (6nm)	14.0	1.019	45.8	6.6	52
Au (6nm)/ LiF (100nm)	13.5	1.035	46.2	6.4	56
Au (6nm)/MoO ₃ (15nm)	5.2	0.929	27.6	1.4	59
MoO ₃ (3nm)/Au(1nm)/Ag(6nm)/MoO ₃ (5nm) ⁵	9.5	0.915	9.9	0.9	71

¹ Average transmittance for the electrode.

3. Perovskite film characterization

Grazing incidence X-ray diffraction (GIXRD)

After the evaporation of the perovskite the films were characterized by using grazing incidence X-ray diffraction (GIXRD). The data were collected at room temperature in the 2θ range 5–50 ° on an Empyrean PANalytical powder diffractometer, using Cu Kα1 radiation. In Figure 2a a typical diffractogram for the thin perovskite layer is shown. Typically four repeated measurements were collected and merged into a single diffractogram. Pawley refinements³, were performed using the TOPAS computer program⁴ and revealed an excellent fit to a one-phase model with a tetragonal cell ($a = 8.80(2)$, $c = 12.57(2)$ Å) and space group $I4/ cm$.

Scanning Electron Microscopy

Perovskite film morphology was investigated using a high-resolution scanning electron microscope (MERLIN, Zeiss) and micrographs were acquired using an in-lens secondary electron detector (Figure 2b).

4. Performance of perovskite solar cells with 70nm Au as cathode

Comparison experiments were performed with the same device structure and perovskite layer thicknesses but using a thicker (70 nm) top electrode. Table S2 summarizes the most important parameters of these cells.

Table S2. Key parameters of perovskite solar cells with the following configuration: ITO/PEDOT:PSS/PolyTPD/Perovskite/PCBM₆₀/Au for different active layer thicknesses.

Perovskite thickness	J_{sc} (mA cm ⁻²)	V_{oc} (V)	FF	PCE (%)	AVT ¹ (%)
40 nm	9.12	1.021	47.2	4.39	45
100 nm	11.36	1.065	58.0	7.02	44
180 nm	18.38	1.082	58.5	11.63	33
250 nm	17.97	1.060	58.4	11.13	19

¹ Average transmittance for the device without the metallic cathode.

The main difference when decreasing the perovskite thickness is the lower current density that the devices produce, as the FF and V_{oc} are almost not affected when using active layers thicknesses above 100 nm. Nevertheless, there is an important decrease for the 40 nm devices, which affects strongly the device performance. The best efficiencies are obtained for 180 nm and 250 nm perovskite films, leading to values of PCE close to 12%. Comparing these results with the obtained for the ST cells it is evident the limitation that the ST electrode may have in the current density during the device operation, lowering the resulting FF. Moreover, the device with 180 nm of active layer shows a high value for PCE and AVT of 33 % without the top electrode. These results suggest that really high efficiencies could be achieved with a proper semitransparent electrode.

5. Transmittance spectra for optimized device

The transmittance spectra through a typical semitransparent solar cell with the best semitransparent electrode (Au/LiF) and 100 nm of perovskite thickness is shown in Figure S2.

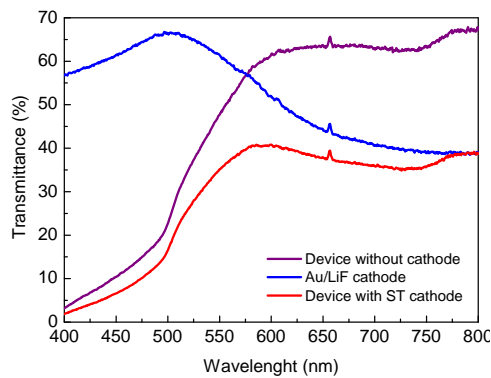


Figure S2. Transmittance spectra for the device without top electrode, the semitransparent (ST) top contact and the completed device with ST top contact using a perovskite layer thickness of 100 nm.

6. Chromaticity coordinates for the semitransparent devices

The color calculation of both actual and simulated devices is based on the determination of the CIE 1931 chromaticity coordinates x and y . Given the devices transmittance $T(\lambda)$ and taking as reference the daytime $D65(\lambda)$ standard illuminant,⁶ the X , Y and Z tristimulus values are calculated as follows:⁷

$$X = \frac{1}{N} \int_{\lambda} \bar{x}(\lambda) T(\lambda) I(\lambda) d\lambda$$

$$Y = \frac{1}{N} \int_{\lambda} \bar{y}(\lambda) T(\lambda) I(\lambda) d\lambda$$

$$Z = \frac{1}{N} \int_{\lambda} \bar{z}(\lambda) T(\lambda) I(\lambda) d\lambda$$

Where $N = \int_{\lambda} \bar{y}(\lambda) I(\lambda) d\lambda$ and $\bar{x}(\lambda)$, $\bar{y}(\lambda)$ and $\bar{z}(\lambda)$ are the CIE standard observer functions. Finally, the chromaticity coordinates are directly calculated as:

$$x = \frac{X}{X + Y + Z}$$

$$y = \frac{Y}{X + Y + Z}$$

Figure S3 shows the CIE (x,y) coordinates calculated for the semitransparent devices using both the transmission spectra of the experimental devices and the predicted ones in the optical modeling.

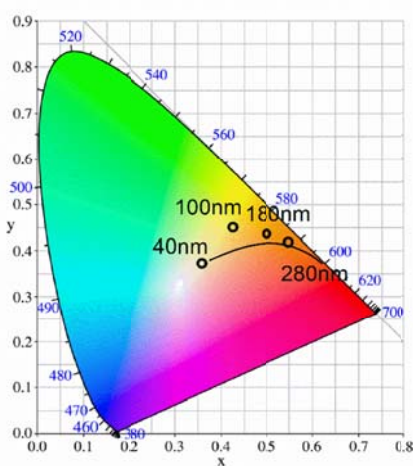


Figure S3. b) CIE 1931 color coordinates calculated using the transmission spectra of the experimental devices (black circles) and the transmission spectra predicted in the optical modelling (solid line).

All devices exhibited a yellowish/brown tonality with considerably good agreement with the optical modelling. The 40 nm thick perovskite device displayed the most neutral color (0.36;0.37) and future works could be addressed to develop optical strategies to tune such tonalities.

Notes and references

1. L. Etgar, P. Gao, Z. Xue, Q. Peng, A. K. Chandiran, B. Liu, M. K. Nazeeruddin and M. Grätzel, *Journal of the American Chemical Society*, 2012, **134**, 17396-17399.
2. O. Malinkiewicz, A. Yella, Y.H. Lee, G. Mínguez Espallargas, M. Grätzel, M. K. Nazeeruddin and H. J. Bolink, *Nature Photonics*, 2014, **8**, 128–132.
3. G. S. Pawley, *J. Appl. Cryst.*, 1981, **14**, 357-361.
4. Coelho, A. A. TOPAS-Academic, Version 4.1, 2007, see: [http:// www.topas-academic.net](http://www.topas-academic.net).
5. S. Schubert, J. Meiss, L. Müller-Meskamp and K. Leo, *Adv. Energy Mater.* 2013, **3**, 438-443.
6. Commission Internationale De L'éclairage. (2013).
7. Betancur, R. (2013). Photon control in nano-structured organic photovoltaic materials (Doctoral dissertation, Universitat Politècnica de Catalunya Barcelona).